Apportioning and Locating PM2.5 Sources Affecting Coastal Cities: Ulsan in South Korea and Dalian in China

Eunhwa Choi, Kwonho Jeon, Young Su Lee, Jongbae Heo, Ilhan Ryoo, Taeyeon Kim, Chuanlong Zhou, Philip K Hopke, Seung-Muk Yi

Aerosol and Air Quality Research

ORIGINAL RESEARCH
https://doi.org/10.4209/aaqr.240031

Apportioning and Locating $PM_{2.5}$ Sources Affecting Coastal Cities: Ulsan in South Korea and Dalian in China

Eunhwa Choi[1], Kwonho Jeon[2], Young Su Lee[3], Jongbae Heo[4], Ilhan Ryoo[5], Taeyeon Kim[5], Chuanlong Zhou[6], Philip K. Hopke[7,8], Seung-Muk Yi[5*]

[1] Research Institute of Industrial Science & Technology, Gyeongsangbuk-do 37673, Korea
[2] Climate and Air Quality Research Department Global Environment Research Division, National Institute of Environmental Research, Incheon, Korea
[3] Department of Energy and Environmental Engineering, Soonchunhyang University, Asan, Korea
[4] Busan Development Institute, Busan 47210, Korea
[5] Department of Environmental Health Sciences, Graduate School of Public Health, Seoul National University, Seoul, Korea
[6] Laboratory for Sciences of Climate and Environment, Gif-sur-Yvette, France
[7] Center for Air Resources Engineering and Science, Clarkson University, Potsdam, New York 13699, USA
[8] Department of Public Health Sciences, University of Rochester School of Medicine and Dentistry, Rochester, New York 14642, USA

ABSTRACT

$PM_{2.5}$ mass and its constituent species were analyzed in two coastal cities (Ulsan, South Korea, and Dalian, China) between July 13, 2018, and September 20, 2019. Ten and nine sources were identified in Ulsan and Dalian, respectively, using positive matrix factorization (PMF). In Ulsan, three sources (secondary nitrate [SN], secondary sulfate [SS], and traffic) contributed ~83.0% of the $PM_{2.5}$ mass concentration (23.7 μg m^{-3}) during the heating period. In Dalian, four sources (SN, SS, traffic, and residential burning) accounted for ~84.3% of the total $PM_{2.5}$ mass concentration (47.8 μg m^{-3}). Higher contributions of residential burning in Dalian (11.7 μg m^{-3}) than biomass burning in Ulsan (0.22 μg m^{-3}) were resolved during the heating period as was a higher proportion of SS contributions in Ulsan (6.28 μg m^{-3}, 41.6%) than in Dalian (6.42 μg m^{-3}, 21.2%) during non-heating period. Squared correlation coefficients (r^2) of sources common to the two cities were examined for lag times from –2 days to +4 days from Dalian to Ulsan. The largest r^2 of $PM_{2.5}$ mass concentrations during the heating period was 0.34 on Lag day 1. The same day, largest r^2 during the non-heating period was 0.14 indicating, stronger, lagged $PM_{2.5}$ correlations during the heating period. The SN, SS, soil, and oil combustion sources, with r^2 values of 0.25, 0.20, 0.41, and 0.25, respectively, show fair correlations between the cities for these sources during the heating period. Probable source locations were identified by simplified quantitative transport bias analysis (SQTBA) and potential source contribution function (PSCF) as a multiple site approach and a single site approach, respectively. Weaker correlations of SN ($r^2 = 0.15$) and SS ($r^2 < 0.1$) during the non-heating period were supported by the different probable source locations. This study identified the sources requiring individual national and/or joint international efforts to reduce ambient $PM_{2.5}$ in these neighboring countries.

Keywords: $PM_{2.5}$, Source apportionment, Positive matrix factorization, Potential source contribution function, Simplified quantitative transport bias analysis

OPEN ACCESS

Received: January 31, 2024
Revised: May 16, 2024
Accepted: May 18, 2024

* **Corresponding Author:**
yiseung@snu.ac.kr

Publisher:
Taiwan Association for Aerosol Research
ISSN: 1680-8584 print
ISSN: 2071-1409 online

1 INTRODUCTION

Air pollution is a significant cause of adverse health outcomes (WHO, 2021). The International Agency for Research on Cancer (IARC) concluded that outdoor air pollution is carcinogenic to humans, with the particulate matter (PM) component of air pollution most highly associated with increased cancer incidence (WHO, 2016). Despite various efforts to improve air quality over the past decades, $PM_{2.5}$ concentrations in many countries still exceed the $PM_{2.5}$ guideline values (5 μg m^{-3} for the annual mean value; 15 μg m^{-3} for the daily mean value) recommended by the WHO (2021).

Because $PM_{2.5}$ can be transported over long distances, neighboring cities and countries and even different continents can be influenced by $PM_{2.5}$ originated from regional sources or transported from distant regions (Perry *et al.*, 1997; VanCuren and Cahill, 2002; Park *et al.*, 2004; Vallius *et al.*, 2005; Uno *et al.*, 2009; Amato *et al.*, 2016; Kim *et al.*, 2022b; Yen *et al.*, 2024). Comparisons of $PM_{2.5}$ concentrations, chemical compositions, and sources measured in many cities across Europe have been reported (Vallius *et al.*, 2005; Sillanpää *et al.*, 2006; Amato *et al.*, 2016). In Asia, long range transport of air pollutants from the Asian continent have been reported in studies conducted in Japan and Taiwan (Lee *et al.*, 2019; Hung *et al.*, 2019; Griffith *et al.*, 2020). Park *et al.* (2018) compared the $PM_{2.5}$ mass concentrations and its major constituents in three East Asian cities: Seoul, South Korea (hereinafter, Korea); Beijing, China; Nagasaki, Japan. Additionally, regionally transported $PM_{2.5}$ from outside of China were identified in Beijing (Wang *et al.*, 2015). Liu *et al.* (2020) estimated that $PM_{2.5}$ pollution from outside China caused 100 thousand premature deaths in 2015, accounting for 9.60% of the $PM_{2.5}$ related premature deaths.

Studies performed in Korea showed that long-range transported $PM_{2.5}$ formed from secondary inorganic precursor sources, or emitted by coal combustion, and industrial sources in China, soil dust from China and Mongolia, and biomass burning in China, Mongolia, and Russia influenced the $PM_{2.5}$ concentrations in Seoul, Incheon, or Daebudo, Korea (Heo *et al.*, 2009; Choi *et al.*, 2013; Kim *et al.*, 2018; Lee *et al.*, 2023). Kim *et al.* (2022b) reported that severe haze in Seoul, Korea during the winter of 2017 was influenced by transported nitrate, sulfate, and ammonium with a high proportion of the $PM_{2.5}$, transported from eastern China. Kim *et al.* (2022a) reported that residential coal combustion in northern China increased $PM_{2.5}$ concentrations in Seoul during the COVID-19 lockdown. Kim *et al.* (2020a) showed that regional transport of polluted air masses likely played an important role in the haze episodes observed in Seoul during early spring based on simultaneous measurements in Seoul (downwind) and Beijing (upwind). Nonetheless, characterization, transport, and source apportionments of atmospheric $PM_{2.5}$ mass concentrations measured during a given period using consistent methods between neighboring countries are very limited.

Most previous studies of $PM_{2.5}$ transported from outside Korea have been done in Seoul or Incheon, located in northwestern Korea and close to China. Ulsan is a city located in the southeast of Korea, and situated east of the Taebaek Mountains that divide Korea's spine from east to west and was considered less vulnerable to pollutants arriving from the northwest. However, according to the Korea Meteorological Administration, over the 30 years from 1991 to 2020, Asian dust was observed in Seoul and Incheon for 29 of those years (96.7%), and in Ulsan, located in southeastern Korea, Asian dust was observed in 26 years (86.7%). The effect of Asian dust observed in Ulsan indicates the likelihood of other transported $PM_{2.5}$ or influencing local concentrations. Korea's main wind pattern changes clearly depending on the season. In winter, cold, and dry northwest winds blow under the influence of continental high pressure. Thus, further studies were needed to determine transported pollutant impacts on southeastern coastal locations in Korea.

Dalian, located in northeastern China (upwind of Ulsan), is a city with high $PM_{2.5}$ concentrations and a moderate economic growth rate (Wang *et al.*, 2023). The $PM_{2.5}$ concentration in Dalian is expected to increase due to fuel combustion during the cold winter. However, compared to cities with higher economic growth rates (e.g., Beijing, Shanghai, Tianjin, and Hebei) in northern China, few studies have been conducted on its atmospheric $PM_{2.5}$ concentrations or sources. Moreover, it has never been compared with the concentrations or sources of $PM_{2.5}$ in Korean cities.

Thus, this study was performed in Ulsan, Korea and Dalian, China. Both are coastal industrial cities, but they have their own characteristics, including geographic location, meteorological

conditions, and local sources of $PM_{2.5}$. This study compared the $PM_{2.5}$ sources and their contributions to these two coastal cities using positive matrix factorization (PMF) and determined the likely $PM_{2.5}$ source regions related to both cities to identify the potential $PM_{2.5}$ abatement opportunities from individual and/or joint efforts. Conditional bivariate probability function (CBPF), correlation analysis of the sources common to the two cities, potential source contribution function (PSCF), and simplified quantitative transport bias analysis (SQTBA) were used to explore the local, regional, and common source locations of $PM_{2.5}$ in Ulsan and Dalian.

2 MATERIALS AND METHODS

2.1 Study Sites

The locations and characteristics of the two study sites are presented in Fig. S1 and Table S1 in supplementary material (SM). The Ulsan site (35°34'52.0''N, 129°19'27.0''E) in Korea is one of intensive air pollution monitoring stations operated by the Ministry of Environment and the National Institute of Environmental Research (NIER) of Korea. Ulsan is situated in southeastern Korea. The sampling site is ~8 km and ~16 km from two large, nationally designated, industrial complexes including petrochemical, non-ferrous metal, car manufacturing, and ship building industries that are known $PM_{2.5}$ sources (Choi *et al.*, 2011). The Dalian site (38°53'10.0''N, 121°34'06.8''E) in China is located in the Shahekou district. It is ~7 km southwest of the center of Dalian and ~2 km from a Dalian high-tech zone (called the Dalian software park) to the east. Port and industrial complexes including machinery, petrochemical, shipbuilding, locomotive manufacturing, and automobile industries are located to the northeast of the sampling site. The two cities are approximately 800 km from each other.

2.2 Sampling and Chemical Analysis

There were differences in the sampling/analysis processes in the two cities. In Ulsan, hourly data were obtained using a set of in situ speciation monitors. Hourly concentrations of organic carbon (OC) and elemental carbon (EC) were collected on a quartz filter and measured by thermal-optical transmittance method (Model-4 Semi-Continuous OC-EC Field Analyzer, Sunset Laboratory Inc., USA). Ionic species (NO_3^-, SO_4^{2-}, Cl^-, Na^+, K^+, and NH_4^+) were measured by Dionex® Ion Chromatography (URG-9000D ambient ion monitor, URG Corp., USA). Elements with atomic numbers $\geq$ 12 were measured by X-ray fluorescence spectrometry (XRF) (XactTM 620, Cooper Environmental Services, USA). $PM_{2.5}$ mass concentration was measured using a MetOne 1020 Beta attenuation monitor (BAM) that has been designated as a $PM_{2.5}$ Federal Equivalent Method (US Federal Register, EQPM-0308-170). In Dalian, multiple integrated filter samples were collected using a $PM_{2.5}$ sampler with three parallel channels at a flow rate of 16.7 L min^{-1}. The filters were analyzed off-line using the gravimetric method (40 CFR 53) for mass and for chemical species as described in Text S1 of the SM.

2.3 Positive Matrix Factorization

PMF is the most widely used source apportionment tool (Paatero and Tapper, 1994; Hopke *et al.*, 2020). EPA PMF 5.0 was applied to the $PM_{2.5}$ mass concentrations and constituents to identify and apportion $PM_{2.5}$ sources (Text S1.2; Table S2). If the concentration were greater than the method detection limit (MDL), associated uncertainties were prepared according to the equation ($Uncertainty = \sqrt{(0.1 \times concentration)^2 + (0.5 \times MDL)^2}$) in the EPA PMF 5.0 user's guide (Norris *et al.*, 2014). The concentration values below the MDL were replaced by half of the MDL, and their uncertainties were set at 5/6 of the MDL. For missing constituent data, the respective geometric mean was used as the mass concentration and four times the geometric mean was used as its uncertainty. The $PM_{2.5}$ mass concentrations were used as the total variable. The total mass concentrations of $PM_{2.5}$ were down-weighted with an uncertainty of four times the mass concentration to ensure that the results of the PMF models were not considerably affected by the $PM_{2.5}$ total mass itself. $PM_{2.5}$ mass closure and ion charge balance were calculated as data screening steps (Lewis *et al.*, 2003; Maxwell-Meier *et al.*, 2004; Sillanpää *et al.*, 2006). In the initial

PMF run, all species were included, and in subsequent runs, poorly fitted species or species with low signal-to-noise ratios (S/N) were removed by setting to "bad" or down-weighted as "weak" (Table S2) (Paatero and Hopke, 2003). As a result, 20 species including total variable $PM_{2.5}$ in 7471 hourly samples in Ulsan and 24 species from 217 23 h integrated samples in Dalian were included in the respective PMF analyses. Because shorter sampling duration provides better factor resolution and increases the number of sources resolved (Lioy *et al.*, 1989), the hourly Ulsan data were used in the PMF analysis.

Source contributions resolved by PMF in Ulsan and Dalian were compared using daily mean values in Ulsan and 23 h-integrated values in Dalian by averaging the hourly source contributions in Ulsan to daily mean values (a total of 369 values). $PM_{2.5}$ mass concentrations increased and $PM_{2.5}$ source contributions changed during the cold season when building heating was implemented. Thus, the analysis of $PM_{2.5}$ mass concentrations and $PM_{2.5}$ source contributions, and the tracing of $PM_{2.5}$ source locations was examined separately for the heating and non-heating periods after the PMF analyses for the entire period. The heating period in Dalian, China was between November 5 and March 31 of the following year. A similar heating season occurred in Ulsan, Korea.

2.4 Statistical Analysis

Data analysis was performed using the Statistical Package for Social Sciences (version 21; IBM Corp., Armonk, NY, USA). The strength of relationships between sources resolved by PMF in Ulsan and Dalian were assessed using squared Pearson's correlation coefficients. High correlations due to similar seasonal pattern in source contributions was minimized by separately analyzing the correlations for the heating period and non-heating period rather than for the entire period. Lag times from Dalian to Ulsan between –2 days and +4 days were used in the correlation analysis. The statistical differences in the contribution of $PM_{2.5}$ sources between heating and non-heating periods were found not to follow a normal distribution. Thus, the differences were assessed using the Mann Whitney U test for pairwise comparisons.

2.5 Conditional Bivariate Probability Function

CBPF analysis (Uria-Tellaetxe and Carslaw, 2014) was applied to the PMF resolved contributions using surface wind directions and speeds (KMA, 2021; Raspisaniye Pogodi Ltd., 2021) to help identity the factors and investigate source directionality (Text S1.3). In this study, 12 sectors ($\Delta\theta$ = 30°) and threshold criteria of the upper 25th percentile for each source contributions were applied. CBPF values were down-weighted by multiplying 0.25, 0.5, and 0.75 when the total numbers of occurrences in particular wind direction-speed interval were 1, 2, and 3, respectively (Carslaw, 2019).

2.6 Potential Source Contribution Function and Simplified Quantitative Transport Bias Analysis

In this study, PSCF analysis was applied to locate possible source areas in the respective city, and SQTBA was applied to explore common regions of the sources extracted in Ulsan and Dalian. PSCF (Ashbaugh *et al.*, 1985) was used to identify $PM_{2.5}$ source regions for each site. PSCF is based on the concept that the regions frequently traversed by high-concentration trajectories are source regions or pathways. Quantitative transport bias analysis (QTBA) was developed by Keeler (1987) as a multiple site approach (Hopke, 2016). QTBA has sophisticated features because normal distribution by atmospheric dispersion is approximated along the trajectory centerline and the standard deviation increases linearly with backward time (Han, 2005; Hopke, 2016). However, it is very difficult to implement. Thus, a practical approach, SQTBA, has been applied using basic framework of QTBA (Zhou *et al.*, 2004; Han, 2005; Hopke, 2016).

The Hybrid Single-Particle Lagrangian Integrated Trajectory (HYSPLIT 5.1) model (Stein *et al.*, 2015) and gridded meteorological data (GDAS1) from the US National Oceanic and Atmospheric Administration were used to calculate air parcel backward trajectories using 0.9 planetary boundary layer (PBL) as starting heights. The GDAS 1 data were selected because of the availability for the study period and its better performance in retrieving contributions from various directions (Su *et al.*, 2015; Park *et al.*, 2024). Source contributions were used as input data in the PSCF and SQTBA

analyses. Four-day backward time was selected to explore regional source areas of $PM_{2.5}$ in Ulsan and Dalian. For PSCF analysis of soil sources, upper 5^{th}–10^{th} percentile concentration criteria were used to locate probable source areas. For the other sources, an upper 25^{th} percentile criterion was applied. Details of the PSCF and SQTBA calculations are presented in Text S1.4 and S1.5. SQTBA used an open-source web application, Trajectory based source apportionment (TraPSA) (Zhou *et al.*, 2024).

3 RESULTS AND DISCUSSION

3.1 Overview of the Observations

$PM_{2.5}$ mass concentrations and constituents (μg m^{-3}) measured in Ulsan and Dalian between July 13, 2018 and September 20, 2019 were compared. In Ulsan, daily mean mass concentration of $PM_{2.5}$ during the entire period was 19.0 ± 12.6 μg m^{-3}, with a range of 2.3–73.0 μg m^{-3}. In Dalian, the 23 h mean $PM_{2.5}$ mass concentration during the entire period was 38.1 ± 28.1 μg m^{-3}, with a range of 8.2 to 188 μg m^{-3} indicating the $PM_{2.5}$ concentration in Dalian was approximately twice that in Ulsan. The 23 h mean value of $PM_{2.5}$ (38.1 μg m^{-3}) measured in Dalian was similar with daily mean value (35.9 μg m^{-3}) measured at the nearest monitoring station for the same measurement period (Fig. S2).

The heating and non-heating seasonal average $PM_{2.5}$ concentrations were 24.8 ± 14.3 μg m^{-3} and 16.0 ± 10.5 μg m^{-3}, respectively, in Ulsan, and 49.6 ± 37.3 μg m^{-3}, 30.4 ± 15.6 μg m^{-3}, respectively, in Dalian (Fig. S2). Therefore, the average $PM_{2.5}$ concentration during the heating period was more than 1.5 times the average $PM_{2.5}$ concentration during the non-heating period in both cities. Higher $PM_{2.5}$ concentrations during the heating period are due to elevated emissions from fossil fuel and biomass burning for heating, poorer atmospheric dispersion, and increased condensation of semi-volatile organic compounds on pre-existing aerosols (Lee and Hieu, 2011; Xie *et al.*, 2019; Dai *et al.*, 2021). Mass concentrations of $PM_{2.5}$ and its chemical composition in Ulsan and Dalian are shown in the Table S2. The $PM_{2.5}$ pollution in both cities are further characterized using PMF in Section 3.2.

3.2 Source Apportionment

PMF solutions were explored from eight to eleven factors for Ulsan and six to ten factors for Dalian. The best fits to the data were chosen by examining the model performance including the distributions of scaled residuals and the interpretability of factors (Paatero *et al.*, 2005) (Table S3). In Ulsan, the number of scaled residuals beyond 3 σ decreased from 158 to seven when factor size increased from nine to ten. In Dalian, the number of scaled residuals beyond 3 σ decreased from ten to three when factor size increased from seven to eight and decreased from three to one when factor size changed from eight to nine. However, the source profiles of vehicle exhaust mixed with industry sources in the eight factor models and there was slight increase in the r^2 between observed and modeled $PM_{2.5}$ in the nine factor model (Table S4). Thus, ten- and nine-factor models were chosen as the optimal fits in Ulsan and Dalian, respectively. The uncertainty of PMF solution associated with the change of source profile were assessed using the displacement (DISP) analysis. Although DISP is very sensitive to higher data uncertainties (Paatero *et al.*, 2014; Brown *et al.*, 2015), the DISP range were distinctly shorter for the marker species for each specific source, indicating little rotational ambiguity in the solutions (Fig. 1). There were no swaps and the bootstrap results conformed with the 80% requirement for correlation with the base run results.

The time series of PMF factor contribution are shown in Fig. 2. The model predicted $PM_{2.5}$ mass concentrations correlated with the observed values with squared correlation coefficients (r^2) of 0.939 and 0.960 for Ulsan and Dalian, respectively.

Secondary nitrate was characterized by the highest fraction of NO_3^- and NH_4^+ with tight DISP intervals and accounted for 30.9% and 30.5% of total $PM_{2.5}$ in Ulsan and Dalian respectively (Fig. 1; Table S5). Higher contribution of SN sources during heating period at both sites may be explained by the formation of particle-phase ammonium nitrate facilitated by low temperature in winter (Peng *et al.*, 2021).

Secondary sulfate comprised the highest fraction of SO_4^{2-} and NH_4^+ occupied the largest

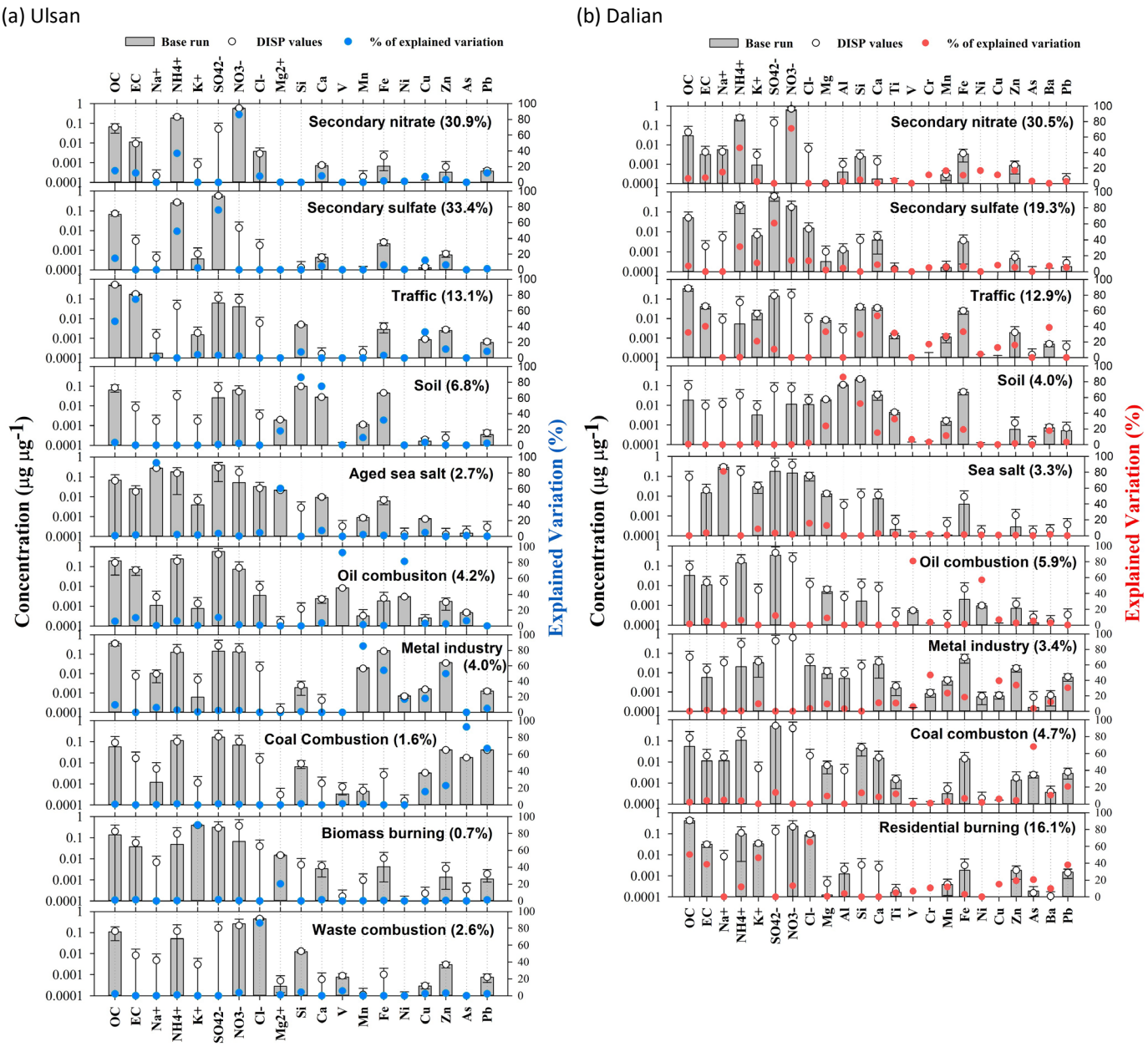

Fig. 1. Profiles of the source factors extracted by PMF: (a) Ulsan; (b) Dalian. The bars represent the concentrations of respective species apportioned to each factor (left axis). The open circles are the mean DISP values and the error bars provide the minimum and maximum DISP values. The filled circles are the percent explained variations (right axis).

portion (33.4%) and the second largest portion (19.3%) of total $PM_{2.5}$ in Ulsan and Dalian, respectively (Table S5). It is known that sulfate concentration is generally high in warm season due to increased photochemical activity (Miyakawa *et al.*, 2007). However, in Dalian, the SS source contribution was higher during heating period although the difference was not statistically significant (Fig. 2). Many studies have reported higher sulfate concentrations during heating period due to domestic coal and biomass burning for heating purpose in Chinese cities (Dai *et al.*, 2019, 2021) and indicated the primary or secondary sulfate as a cause of the severe haze during winter (Wang *et al.*, 2016; Dai *et al.*, 2021). Higher concentrations of SO_2 and NO_2 in Dalian during heating period were observed compared to the non-heating period (Fig. S2) implying the possibility of an elevated secondary sulfate concentration downwind and primary sulfate emissions from local residential heating (Dai *et al.*, 2019).

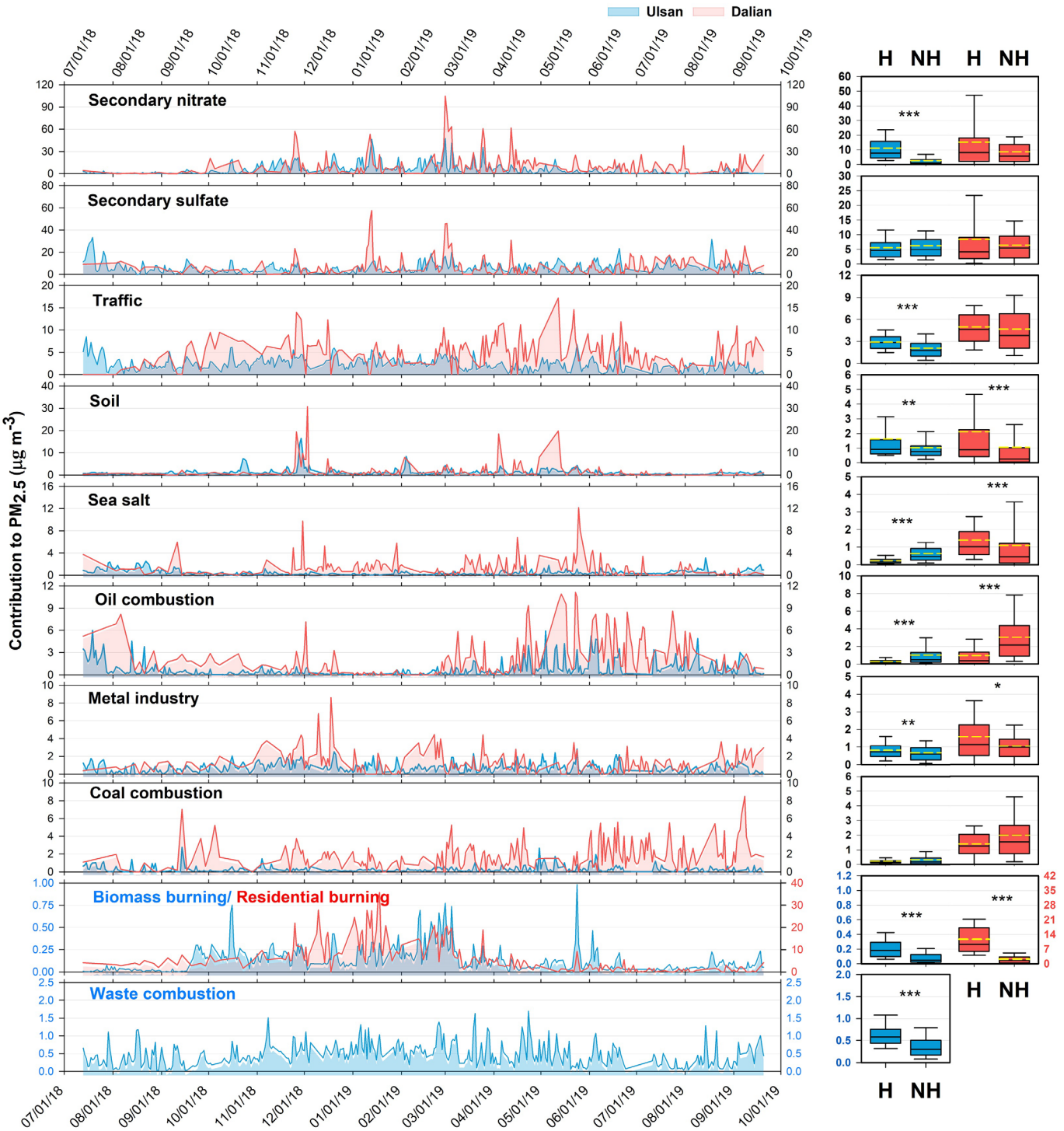

Fig. 2. Daily mean $PM_{2.5}$ mass concentration by source at study sites. Daily mean $PM_{2.5}$ mass concentration in Ulsan and 23 h integrated $PM_{2.5}$ mass concentration in Dalian were used. H and NH denote heating and non-heating period, respectively. Mann Whitney test *p*-values: **p* < .05; ***p* < .01; ****p* < .001.

The traffic related sources, including both exhaust and non-exhaust emissions, contained high concentrations of OC, EC, Fe, Zn, Pb, Ti (Liu *et al.*, 2014; Zannoni *et al.*, 2016). Brake pads and tire wear are known sources of Mn, Zn, Fe, and Ti (Apeagyei *et al.*, 2011; Zannoni *et al.*, 2016). The presence of Pb and Ti is attributed to the ablation of road paint (Yu *et al.*, 2016; Zannoni *et al.*, 2016). Ba, Ca, and Mg shown in Dalian's source profile are used in lubricating oil additives (Whisman

et al., 1974). This source made up 13.1% and 12.9% of total $PM_{2.5}$ mass concentration in Ulsan and Dalian respectively.

The soil source was dominated by typical crustal components such as Si, Fe, Ca, Al, Mg, and Ti (Vouk and Piver, 1983). Higher contribution of soil source during heating period was observed in both cities and statistically significant in Ulsan ($p < 0.01$) and in Dalian ($p < 0.001$). Ulsan was affected by Asian dust events between November 28 and 30, 2018 (KMA, 2022). A severe haze-fog episode was reported over North China between November 23–26 (Tang *et al.*, 2020). The daily mean $PM_{2.5}$ concentrations in Ulsan were 29–54 μg m^{-3} (November 28 to 30) and that in Dalian was 122.6 μg m^{-3} (November 26) (Fig. 2). The $PM_{2.5}$ mass concentration of the soil source resolved with PMF was 9.4–16.4 μg m^{-3} in Ulsan (November 28 to 30) and 19.4 μg m^{-3} in Dalian (November 26) (Fig. S3). In addition to the days recorded as Asian dust events in Ulsan, there were days when the soil source contributions in Ulsan increased after those in Dalian increased.

The sea salt source was identified by Na^+, Ca, Cl^-, or Mg/Mg^{2+} (Enghag, 2008). This source comprised 0.49 μg m^{-3} in Ulsan and 1.21 μg m^{-3} in Dalian for the entire period (Table S5). The higher contribution in Dalian can be due to the sampling site being closer to the sea (approximately 1 km) compared to Ulsan site (11 km) (Fig. S1).

The oil combustion source was indicated by high explained variations and tight DISP intervals of V and Ni, elements characteristic of heavy fuel or residual oil combustion (Vouk and Piver, 1983; Jang *et al.*, 2007; Anastasopolos *et al.*, 2023). This source can be attributed to marine diesel emissions from ships in the ports, or in nearby shipping lanes (Agrawal *et al.*, 2008a, 2008b, 2009, 2010; Shanavas *et al.*, 2020) as well as emissions from petrochemical plants, refineries, or oil-fired industrial boilers in Ulsan and Dalian (Choi *et al.*, 2021; Zhao *et al.*, 2021). The higher contributions during the non-heating period suggest that this source is more influenced by ship emissions than point sources. The $PM_{2.5}$ concentration from oil combustion was significantly higher ($p < 0.001$) during non-heating period than during heating period in both cities. While petrochemical production is relatively constant throughout the year, ship entries and departures in Korea during non-heating period was distinctly higher between 2015 and 2019 (Statistics Korea, 2022). Similarly, the volume of freight handled in coastal ports in China was larger during non-heating period between Mar. 2021 and Feb. 2022 (National Bureau of Statistics of China, 2022) and these were compatible with automatic identification system maritime data (UCL Energy Institute, 2021).

The next sources were related to the metal related industrial activities. The profiles in Ulsan were characterized by high contributions of OC and narrow DISP intervals of Fe, Zn, Mn, Cu, and Pb whose dominant sources are ferrous and non-ferrous metal industries (Dai *et al.*, 2015). The profile of the metal industry in Dalian was dominated by Fe, Zn, Mg, Ca, Pb, Mn, and Cu with small contributions of OC or SO_4^{2-}, and NO_3^- indicating the impact of metal processing industries rather than metal production or smelting (Fig. 1 and Fig. S1).

The coal combustion source featured high loadings of SO_4^{2-} and NH_4^+ and high explained variations of As and Pb (Tian *et al.*, 2014; Yu *et al.*, 2016). While coal is used mostly in coal fired power plants or industrial plants for metal smelting in Korea, coal consumption for residential heating/cooking purposes is still widely used (Kim *et al.*, 2020b) and is very common in China (Tian *et al.*, 2015; Li *et al.*, 2019; Hopke *et al.*, 2020; Dai *et al.*, 2021, 2023). However, higher emissions of As and Pb from coal consumption was attributed to coal fired power plants or industrial boilers rather than residential sectors in China (Tian *et al.*, 2015). Additionally, increase in the contribution of this source in Dalian from March to September (Fig. 2) suggested that this was attributed to not only electricity generation for district heating or industrial boilers but also to electricity generation for space cooling. Rapid rise in space cooling demands in China (IEA, 2019) explain the higher proportion of this sources during non-heating period.

The next factor in Ulsan was interpreted as biomass burning because it featured high explained variations of K^+ and high loadings of OC, EC, and SO_4^{2-} (Hopke *et al.*, 2020). The waste combustion source in Ulsan was indicated by OC, Cl^-, NO_3^-, Si, Zn, and Pb (Jayarathne *et al.*, 2018; Kumar *et al.*, 2018; Moffet *et al.*, 2008; Yang *et al.*, 2016). The amount of municipal solid waste combusted nationwide in Korea is usually larger during non-heating period than heating period (Korea Environment Corporation, 2017), but the increase in the contribution of waste combustion source during heating period could be due to industrial incineration and greater partitioning of gas-phase HCl to particulate matter in colder season (Gunthe *et al.*, 2021).

The last factor in Dalian was interpreted as residential burning sources because of high loadings of OC, EC, NO_3^-, K^+, NH_4^+, and Cl^-. The profile was characterized by high explained variations of OC, EC, K^+, which are dominant markers of biomass burning, as well as high variations in As and Pb, coupled with high contributions of Cl^-, a strong marker for coal combustion in China (Yu *et al.*, 2013; Liu *et al.*, 2018). Increased emissions from residential biomass and coal burning during heating period in China has been reported in many previous studies (Li *et al.*, 2019; Dai *et al.*, 2019, 2020, 2021; Hopke *et al.*, 2020). Residential briquetted or lump coal combustion produces primary sulfate (Dai *et al.*, 2019) and significant quantities of OC including humic-like substances (HULIS) (Li *et al.*, 2019). Meanwhile, Cl^- also is a marker of waste combustion (Jayarathne *et al.*, 2018; Li *et al.*, 2012) because of wastes containing plastics made of polyvinyl chloride and the salt in kitchen waste (Yang *et al.*, 2016), and chloride was most associated with district coal combustion in China (Liu *et al.*, 2018; Li *et al.*, 2019). It indicated the possibility of mixed residential burning of coal/biomass/waste and district coal combustion during the heating season. The contribution of this source to $PM_{2.5}$ concentrations in Dalian during the heating period (11.7 μg m^{-3}, 24.4% of $PM_{2.5}$ mass concentration) was significantly higher ($p < 0.001$) compared to that during non-heating period (2.21 μg m^{-3}, 7.3% of $PM_{2.5}$), and markedly higher than biomass burning sources in Ulsan during heating period (0.22 μg m^{-3}, 0.9% of $PM_{2.5}$).

In Ulsan, three sources (SN, SS, and traffic) accounted for approximately 83.0% of $PM_{2.5}$ concentration during the heating period. In Dalian, four sources (SN, SS, traffic, and residential burning) constituted approximately 84.3% of $PM_{2.5}$ concentration during the heating period. SS was a large fraction of $PM_{2.5}$ in Ulsan (33.4%) compared to Dalian (19.3%) during the study period. Thus, there is a need for SS precursor reductions in the Ulsan source areas. During the heating period, the contributions of residential burning sources accounted for 24.4% in Dalian, becoming the second largest source of $PM_{2.5}$ in Dalian.

3.3 Correlations of $PM_{2.5}$ Sources Common to Ulsan and Dalian

$PM_{2.5}$ sources can be local, regional, or both. To identify the local and regional sources that likely influenced the $PM_{2.5}$ mass concentrations in both cities, correlations between the contributions from the sources common to Ulsan and Dalian were analyzed. For residential burning sources in Dalian, correlations with Ulsan's biomass burning, coal combustion, and waste combustion were analyzed. Because there was no notable difference in the correlation coefficients, the correlation with the biomass burning sources in Ulsan is shown (Fig. 4).

The r^2 value indicates the variance of one variable that can be explained by the other variable. During the heating period, the largest r^2 for $PM_{2.5}$ concentrations between the two cities for a +1 day lag was 0.34. Thus, 34% of the variance in $PM_{2.5}$ concentration in Ulsan can be explained by the changes in $PM_{2.5}$ concentration in Dalian with a one-day transport period. However, during the non-heating period, the largest r^2 of $PM_{2.5}$ concentration was 0.14 on the same day, indicating a weak correlation during the non-heating period. The r^2 of SN (0.25), SS (0.20), soil (0.41), and oil combustion (0.25) sources were > 0.2 during the heating period. However, the r^2 of SN (0.15), SS (0.08), and oil combustion (0.18) were < 0.2 during the non-heating period. Soil had a r^2 of 0.25 during the non-heating season. The relatively higher r^2 of soil sources is probably due to when a combination of wind erosion of cultivated soil and dust storms would affect both cities. A dust storm in the Gobi Desert on April 28, 2019 was reported, and Asian dust events were recorded in six cities (or islands) in Korea between May 1 to 2 (Kai *et al.*, 2021; KMA, 2022).

Given that the relatively higher correlations between sources common to Ulsan and Dalian (SN, SS, soil, and oil combustion sources) can be due to transport on a regional scale as well as local sources, the correlation coefficients may be somewhat underestimated or overestimated. This possibility arises because $PM_{2.5}$ undergoes various physical and chemical interactions and transformations including phase transitions, gas uptake, and chemical reactions (Monks *et al.*, 2009). There also can be sufficient local source contributions to distort the covariances.

The SN, SS, soil, and oil combustion sources with relatively higher correlation coefficients between Ulsan and Dalian had similar fractions of key indicator elements with tight DISP intervals (Fig. 1). In contrast, the sources (traffic, sea salt, and industry) with relatively lower correlation coefficients between the two cities showed respective profile characteristics as explained in 3.2. The coal combustion sources in Ulsan and Dalian showed different Zn, As, and Pb concentrations,

suggesting the differences in coal fuel or burning conditions in the respective cities.

3.4 Local Characteristics of $PM_{2.5}$ Sources

Wind roses, CBPF plots, and Pearson's correlations between secondary and primary sources at Ulsan and Dalian, respectively, are presented in Figs. S4–S7. The CBPF plots for SN and SS sources and high correlations with primary sources in Ulsan compared to in Dalian suggested that SN and SS in Ulsan were more influenced by local sources (Figs. S5–S7). The probable source directions in the SN CBPF plots in Ulsan during the heating and non-heating periods were similar to the four combustion sources (oil, coal, waste, and biomass burning sources), industry, and traffic sources. This directionality indicated the possibility of multiple collocated sources or nitrate formation by the oxidation of NO_x, which is mainly emitted from the combustion sources. The CBPF results in Dalian showed that wind from the southwest direction primarily affected the increase in SN source contributions. Relatively high correlations with coal combustion and residential burning were identified. Such correlations are reasonable given that they would all be NO_x sources that can be rapidly converted to nitrate.

The CBPF results for SS sources showed that the Ulsan site during non-heating period was primarily affected from the southeast where ports and industrial complexes are located. Marine diesel engines are a source of primary sulfate as well as SO_2 (Kim and Hopke, 2008). Higher CPF values under southeasterly winds of 2–4 m s^{-1} during the non-heating period suggested local sources such as emissions from ships (r^2 = 0.31) in the ports and from cargo loading vehicles (r^2 = 0.35) to and from industrial complexes and ports (Figs. S5–S7). In Dalian, the port and most of local industrial sources are northeast of the sampling site (Fig. S1). The elevation in $PM_{2.5}$ mass concentrations during heating period, influenced by SS sources, may be attributed to the port of Dalian and the extensive shipping in the Bohai Sea when the northeasterly wind is strong, at approximately 10 m s^{-1} (Fig. S5). Additionally, an r^2 of 0.32 between SS and residential burning sources suggested that local residential heating contributed to the elevation of SS source contributions during the heating period (Fig. S7). Similarly, the source directions of SS and r^2 = 0.51 with biomass burning at the Ulsan site during heating period indicated that primary sulfate from local burning of biomass could be sources of SS (Dai *et al.*, 2019; Song *et al.*, 2024) (Fig. S5).

The traffic sources affected by ubiquitous local emissions were seen in the Ulsan CBPF plots. Dominant directions of traffic sources were not found because high CBPF values were in the center of the CBPF plots with 0–4 m s^{-1} wind speeds. The ancillary directions of traffic sources were found to be junctions of highways to the east, southwest, and west of the Ulsan site. For Dalian, the CBPF plot showed traffic sources in all directions except to the south and southeast toward the sea.

The CBPF plots, which indicate the direction of relatively local soil sources, pointed southwest of the Ulsan site with wind speed of 7–8 m s^{-1} during the heating period. It was inferred that the site was affected by agricultural activities such as clearing fields or preparing the soil for planting crops in small farmlands to the southwest of the sampling site. The CBPF results for soil at Dalian site during heating period showed that prevailing directions were north and northeast, under strong wind speeds (> 8 m s^{-1}). It appears to be due to agricultural areas in the Ganjingzi district in Dalian.

At both sites, the easterly wind in Ulsan and the southerly wind in Dalian coinciding with the sea direction, prevailed during non-heating period compared to heating period (Fig. S4). This appears to have influenced that the potential source direction of sea salt and oil combustion sources more pronounced during the non-heating period (Fig. S5). The CBPF plots for oil combustion sources at Ulsan showed that prevailing directions was southeast with 0–5 m s^{-1} wind speed. In Ulsan, two ports located at 7.5 km and 13.5 km southeast of the sampling site and the second largest petrochemical complex in Korea to the southeast of the sampling site likely contributed to the oil combustion sources. For Dalian, the CBPF results suggest that oil combustion contributions were from south toward the sea (Fig. S5). The direct southerly and southeasterly directions in both seasons suggest the influence of the major marine shipping lanes that run to Tianjin and Dalian.

Industrial sources were identified near the Ulsan sites to the southeast where Mipo and Onsan industrial complexes are located. In Dalian, the north and northeast where multiple metal processing plants were located, were dominant source directions with 0–8 m s^{-1} wind speeds.

The CBPF results for coal combustion at Ulsan demonstrated southeasterly sources where the

industrial complexes including non-ferrous metal manufacturing plants using coal for smelting, are located. For Dalian, the direction of coal combustion sources during non-heating period included the north and northeast where coal fired power plants are located (Global Energy Monitor, 2022). Additionally, CBPF plots show areas to the south. District space heating or cooling in nearby large residential districts and the Xinghai park is likely influence high CPF values during heating and non-heating periods (Fig. S5).

Biomass burning sources in Ulsan during heating period were identified in the east to northeast where vegetable and horticultural farms are located. In Korea, burning crop residues or weeds on farmland is legally prohibited. From December 1 to March 31 each year, the collection and disposal of agricultural waste has been enhanced as part of the seasonal intensive management program for $PM_{2.5}$. However, there are still some areas where the practice of open burning continues. Households where biomass is used for heating or cooking are rarely found in Korea. As of 2019, the number of households using briquettes in Ulsan is 0.026% of the total number of households (Babsang Community Briquette Bandk and Briquette Bank National Council, 2022). Residential burning sources were only identified at Dalian. During heating period, this source is affected by a very localized emissions as it has high CBPF values in most directions including the center of the plot (low wind speeds) and from the west where the nearest residential district is located.

3.5 Probable Source Region Located by PSCF and SQTBA

The PSCF plots suggest the probable $PM_{2.5}$ source regions for Ulsan and Dalian sites. The sources that were commonly interpretable by the PSCF plots for Ulsan and Dalian were coal combustion, SN, SS, soil, and oil combustion sources (Figs. S8–S9). Among them, probable areas of coal combustion sources for Ulsan and Dalian were not close to each other. In Ulsan, a probable source area of coal combustion was identified along the east coast of Korea including Donghae, Samchok, and Yeongdong where coal-fired power plants are located (Global Energy Monitor, 2022). In Dalian, a probable source area was between southern Shandong Province and Shanghai along the Chinese coast.

Because the PSCF plots showed similar source locations (Figs. S8–S9) for the SN, SS, soil, and oil combustion sources with $r^2 > 0.14$, these joint sources were further assessed using the SQTBA plots (Fig. 4). The SN source areas common to Ulsan and Dalian were in Shandong, Hebei, Henan, and Jiangsu Provinces. Ammonium nitrate is formed in areas characterized by high ammonia and nitric acid concentrations (Lee *et al.*, 2006). Regional transport of high ammonia emissions from agricultural areas in Shandong, Anhui, Jiangsu, Henan, and Hebei (Kim *et al.*, 2006; Lee *et al.*, 2006) and NO_x emissions from high vehicle populations or industrial activities in Shandong, Henan, Hebei, and Jiangsu (Park *et al.*, 2024) likely contribute to NH_4NO_3 concentration in Ulsan and Dalian. In addition, high nitric acid from atmospheric processing of local emissions of NO_x from traffic emissions and industrial facilities in Ulsan and Dalian contribute.

The SQTBA plots show probable common source locations for SN and SS during the heating period and SN during the non-heating period (e.g., Shandong, Hebei, Henan, and Jiangsu) (Fig. 4). The PSCF plots suggest SN and SS in Ulsan were less influenced by China during the non-heating period (Figs. S8–S9). The differences in common source location between heating and non-heating period were greater for SS than SN consistent with lower maximum r^2 values for SN (0.15) and SS (0.08) sources during the non-heating period compared to heating period values (0.25 for SN; 0.20 for SS) (Fig. 3). Lower r^2 values (0.08) of SS sources during the non-heating period support the spread of probable common source regions in Fig. 4 by including the Yellow Sea and the East China Sea. The probable location of SS sources in the sea may represent the oxidation of dimethyl sulfide, ship emissions, and power plants and industrial emissions located along China's coast (Kim and Hopke, 2008; Heo *et al.*, 2009). During the heating period, pollutant emissions from combustion in China may contribute to secondary aerosol formation (Liu *et al.*, 2018; Dai *et al.*, 2019, 2021), resulting in the higher correlations of the SN and SS sources between Ulsan and Dalian, and the common source areas in China identified by SQTBA. Higher correlation of SN and SS on the same days in Ulsan and Dalian (Fig. 3) may be attributed to seasonal variation or meteorological conditions in part (Peng *et al.*, 2021; Miyakawa *et al.*, 2007). Other previous studies (Li *et al.*, 2019; Islam *et al.*, 2023; Chen *et al.*, 2020) also suggested that factors such as geographic location, similar emission characteristics, or seasonal variations in human activities may affect PM variations.

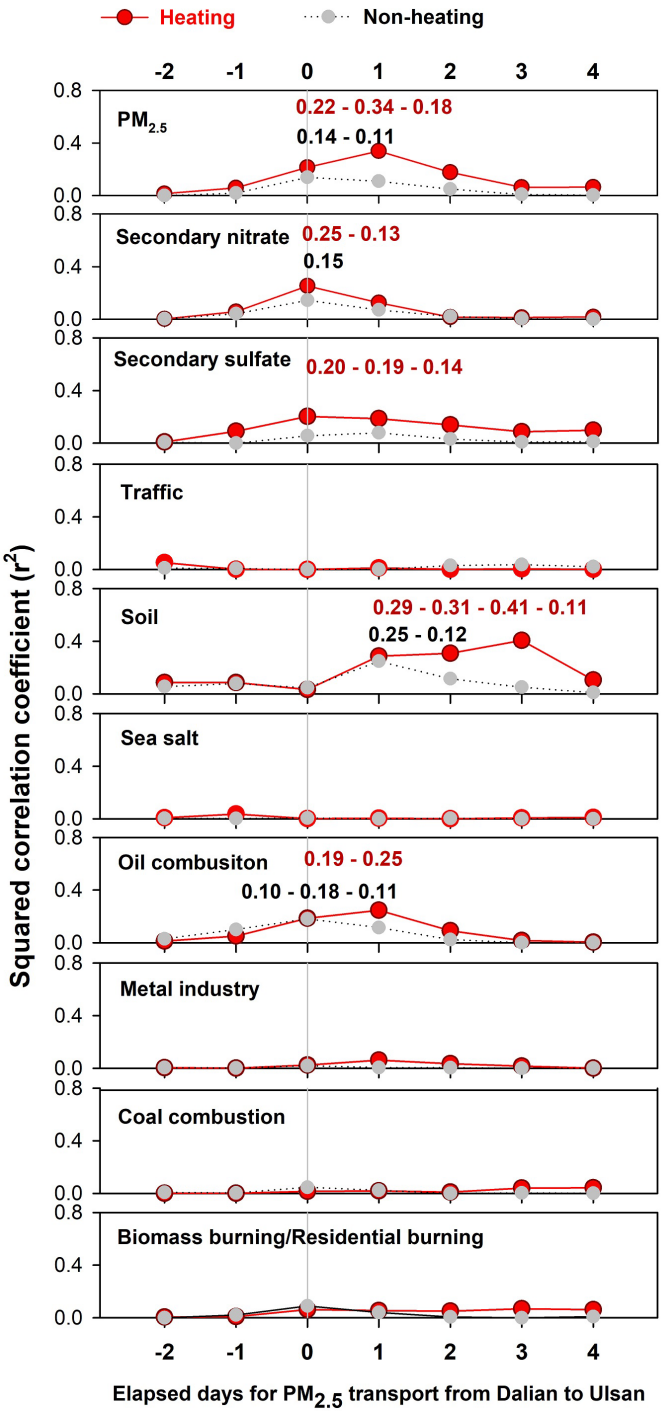

Fig. 3. Squared correlation coefficients (r^2) between common sources to Ulsan and Dalian during heating period and non-heating period. r^2 values larger than 0.1 are presented for each source.

The PSCF plots for the upper 10th percentile of soil source concentration during the heating period in Ulsan and Dalian indicated Mongolia to northern/northeastern China as probable source areas. Asian dust storms occur in dry late winter and spring as air masses move from Mongolia or northern China to the East China Sea (Tan *et al.*, 2017), affecting Chinese and Korean cities (Heo *et al.*, 2009; Choi *et al.*, 2013; KMA, 2022). Trajectories associated with the upper two percentile of hourly soil source concentration in Ulsan showed air parcels (Fig. S11) passing through the Gobi Desert, southern Mongolia, northern China, and Inner Mongolia. The SQTBA plots identified soil sources in similar areas and Shandong province as probable common source areas. A review of 39

(a) Secondary nitrate

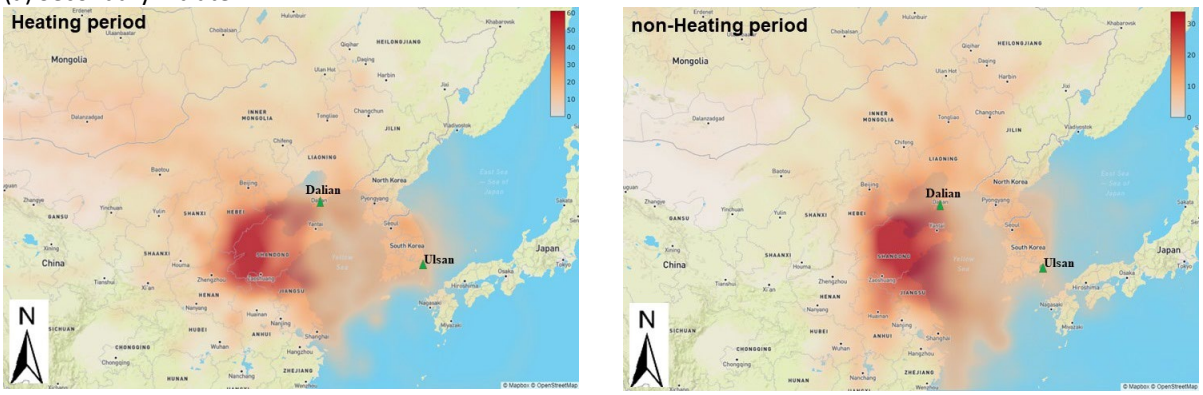

(b) Secondary sulfate

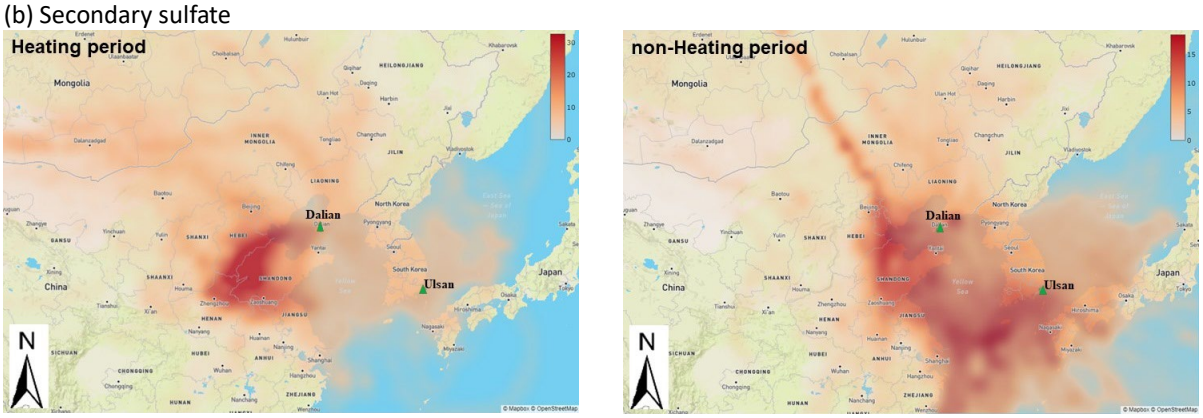

(c) Soil

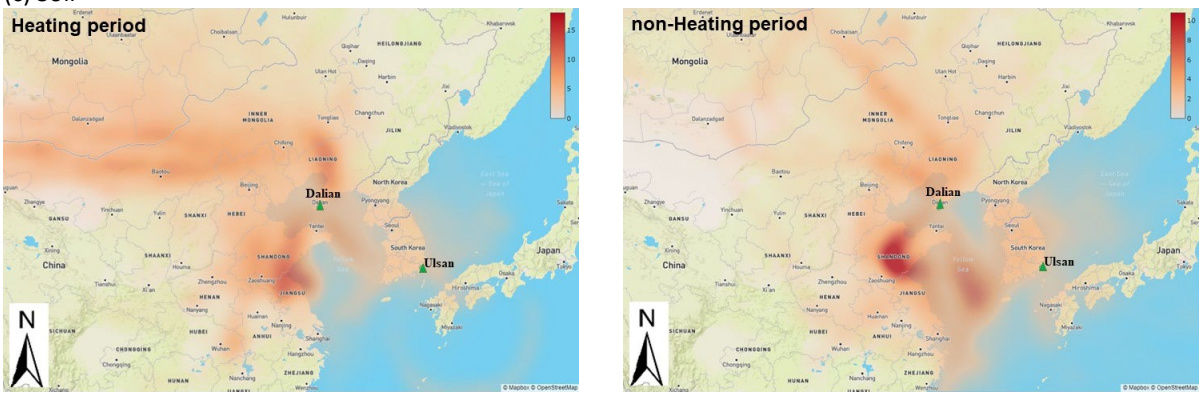

(d) Oil combustion

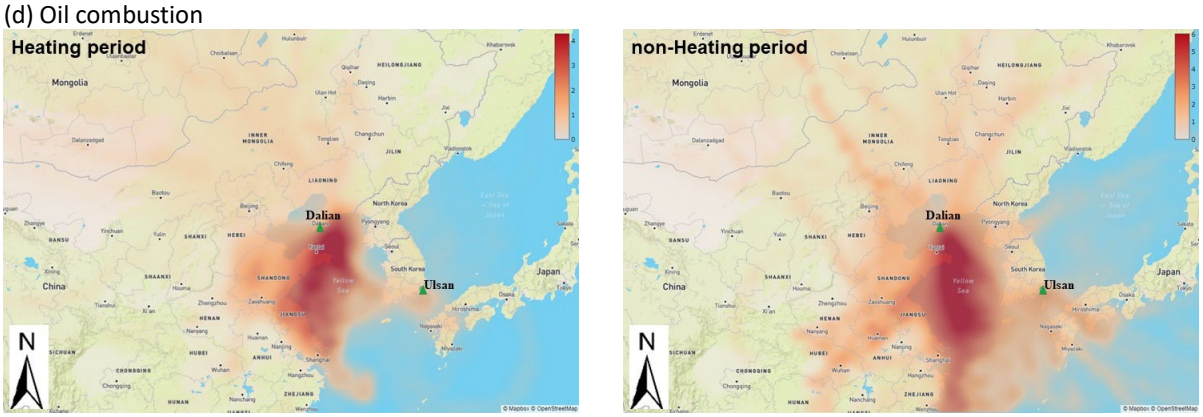

Fig. 4. Likely common source areas identified using SQTBA plots, 96 h backward time during heating and non-heating period: (a) Secondary nitrate; (b) Secondary sulfate; (c) Soil; (d) Oil combustion. (The units of the numbers in the color bar are the weighted SQTBA values.)

studies in Shandong reported dust sources as the second largest PM source accounting for 18.4% of total $PM_{2.5}$ concentration among secondary aerosols, dust, coal combustion, and vehicle emissions (Zhou *et al.*, 2021). Soil and construction dust contributed 11.5% and 7.7%, respectively, to total $PM_{2.5}$ mass concentration (100.9 μg m^{-3}) in Heze, Shandong (Liu *et al.*, 2017). The PSCF plots for soil sources showed the influence of Shandong province on Ulsan and Dalian (Figs. S8–S9).

The PSCF results for oil combustion at Ulsan showed that during heating period, areas near the Yellow Sea contributed marine diesel oil combustion emissions from the extensive shipping in this area. During non-heating period, southerly winds were prevalent such that the probable source region was the East China Sea (Figs. S8–S9). For Dalian, potential source regions identified by PSCF plots were the Yellow Sea during non-heating period and during heating period, were the areas between Shanghai and Qingdao where the world's largest and the seventh largest port, respectively, are located (World Shipping Council, 2020). Joint source areas of oil combustion identified by SQTBA were similar to those identified by the PSCF at Ulsan. Oil combustion was attributable in part to local petrochemical plants, but also from emissions from maritime transport.

4 CONCLUSIONS

Using the $PM_{2.5}$ mass concentration and chemical constituents from Ulsan and Dalian, PMF resolved ten sources in Ulsan and nine sources in Dalian. Similar source types were resolved in both countries. The high emissions and the transport patterns during the heating period led to higher lagged correlations between the cities for the SN, SS, soil, and oil combustion sources implying the $PM_{2.5}$ transport from China to Ulsan in Korea. Comparisons of the r^2 of these common sources and the potential source locations using PSCF and SQTBA plots suggested that the sources with higher correlations (SN, oil combustion, and soil during both heating and non-heating period; SS during heating period) had similar potential source regions. During the non-heating period, scattered potential SS source regions in the SQTBA plots were consistent with the smaller r^2 values. The Ulsan SS source had a common source area with Dalian in China during heating period. The high fractional SS contributions (41.6%) in Ulsan during the non-heating period compared to heating period (23.5%) in Ulsan, and relatively higher correlations among the primary sources (oil combustion and traffic) in Ulsan than those in Dalian suggested the local source management could reduce the Ulsan sulfate concentrations during the non-heating period.

In Dalian, higher SS concentrations (8.4 μg m^{-3}) during the heating period compared to the non-heating period (6.4 μg m^{-3}), and higher r^2 values (0.32) with residential burning sources compared with other primary sources during the heating period were identified. During the heating period in Dalian, residential burning sources and SS sources showed a concentration of 11.7 μg m^{-3} and 8.4 μg m^{-3}, respectively, thus management of residential burning sources could be an effective tool for local and regional air quality management.

The $PM_{2.5}$ source apportionments and the relationships among the two cities common sources showed when and which sources require local national and/or joint international efforts to reduce $PM_{2.5}$ concentrations in these neighboring countries.

ACKNOWLEDGMENTS

This work was supported by a grant from the National Institute of Environmental Research (NIER), funded by the Ministry of Environment (MOE) of the Republic of Korea (No. NIER-2019-04-02-039). Also, this research was supported by Particulate Matter Management Specialized Graduate Program through the Korea Environmental Industry & Technology Institute (KEITI) funded by the Ministry of Environment (MOE).

ADDITIONAL INFORMATION AND DECLARATIONS

Disclaimer

The authors declare that they have no known competing financial interests or personal

relationships that could have appeared to influence the work reported in this paper.

Supplementary Material

Supplementary material for this article can be found in the online version at https://doi.org/10.4209/aaqr.240031

REFERENCES

Agrawal, H., Malloy, Q.G.J., Welch, W.A., Wayne Miller, J., Cocker, D.R. (2008a). In-use gaseous and particulate matter emissions from a modern ocean going container vessel. Atmos. Environ. 42, 5504–5510. https://doi.org/10.1016/j.atmosenv.2008.02.053

Agrawal, H., Welch, W.A., Miller, J.W., Cocker, D.R. (2008b). Emission measurements from a crude oil tanker at sea. Environ. Sci. Technol. 42, 7098–7103. https://doi.org/10.1021/es703102y

Agrawal, H., Eden, R., Zhang, X., Fine, P.M., Katzenstein, A., Miller, J.W., Ospital, J., Teffera, S., Cocker, D.R.I. (2009). Primary particulate matter from ocean-going engines in the Southern California Air Basin. Environ. Sci. Technol. 43, 5398–5402. https://doi.org/10.1021/es8035016

Agrawal, H., Welch, W.A., Henningsen, S., Miller, J.W., Cocker III, D.R. (2010). Emissions from main propulsion engine on container ship at sea. J. Geophys. Res. 115, D23205. https://doi.org/10.1029/2009JD013346

Amato, F., Alastuey, A., Karanasiou, A., Lucarelli, F., Nava, S., Calzolai, G., Severi, M., Becagli, S., Gianelle, V.L., Colombi, C., Alves, C., Custódio, D., Nunes, T., Cerqueira, M., Pio, C., Eleftheriadis, K., Diapouli, E., Reche, C., Minguillón, M.C., Manousakas, M.I., *et al.* (2016). AIRUSE-LIFE+: a harmonized PM speciation and source apportionment in five southern European cities. Atmos. Chem. Phys. 16, 3289–3309. https://doi.org/10.5194/acp-16-3289-2016

Anastasopolos, A.T., Hopke, P.K., Sofowote, U.M., Mooibroek, D., Zhang, J.J.Y., Rouleau, M., Peng, H., Sundar, N. (2023). Evaluating the effectiveness of low-sulphur marine fuel regulations at improving urban ambient $PM_{2.5}$ air quality: Source apportionment of $PM_{2.5}$ at Canadian Atlantic and Pacific coast cities with implementation of the North American Emissions Control Area. Sci. Total Environ. 904, 166965. https://doi.org/10.1016/j.scitotenv.2023.166965

Apeagyei, E., Bank, M.S., Spengler, J.D. (2011). Distribution of heavy metals in road dust along an urban-rural gradient in Massachusetts. Atmos. Environ. 45, 2310–2323. https://doi.org/10.1016/j.atmosenv.2010.11.015

Ashbaugh, L.L., Malm, W.C., Sadeh, W.Z. (1985). A residence time probability analysis of sulfur concentrations at grand Canyon National Park. Atmos. Environ. 19, 1263–1270. https://doi.org/10.1016/0004-6981(85)90256-2

Babsang Community Briquette Bandk, Briquette Bank National Council (2022). 2019 National Briquette Use Household Survey and Proposal. Babsang Community Briquette Bandk. http://www.babsang.or.kr/story/library.php?ptype=view&idx=14896&page=1&code=library

Brown, S.G., Eberly, S., Paatero, P., Norris, G.A. (2015). Methods for estimating uncertainty in PMF solutions: Examples with ambient air and water quality data and guidance on reporting PMF results. Sci. Total Environ. 518–519, 626–635. https://doi.org/10.1016/j.scitotenv.2015.01.022

Carslaw, DC. (2019) The openair manual – open-source tools for analyzing air pollution data. Manual for version 2.6-6, University of York, USA.

Chen, Z., Chen, D., Zhao, C., Kwan, M.P, Cai, J., Zhuang, Y., Zhao, B., Wang, X., Chen, B., Yang, J., Li, R., He, B., Gao, B., Wang, K., Xu, B. (2020). Influence of meteorological conditions on $PM_{2.5}$ concentrations across China: A review of methodology and mechanism. Environ. Int. 139, 105558. https://doi.org/10.1016/j.envint.2020.105558

Choi, E., Heo, J.B., Hopke, P.K., Jin, B.B., Yi, S.M. (2011). Identification, apportionment, and photochemical reactivity of non-methane hydrocarbon sources in Busan, Korea. Water Air Soil Pollut. 215, 67–82. https://doi.org/10.1007/s11270-010-0459-0

Choi, J., Heo, J.B., Ban, S.J., Yi, S.M., Zoh, K.D. (2013). Source apportionment of $PM_{2.5}$ at the coastal area in Korea. Sci. Total Environ. 447, 370–380. https://doi.org/10.1016/j.scitotenv.2012.12.047

Choi, W.J., Jung, B., Lee, D., Kang, H., Kim, H., Hong, H. (2021). An investigation into the effect of

emissions from industrial complexes on air quality in the Ulsan metropolitan city utilizing trace components in $PM_{2.5}$. Appl. Sci. 11, 10003. https://doi.org/10.3390/app112110003

Dai, Q.L., Bi, X.H., Wu, J.H., Zhang, Y.F., Wang, J., Xu, H., Yao, L., Jiao, L., Feng, Y.C. (2015). Characterization and source identification of heavy metals in ambient PM_{10} and $PM_{2.5}$ in an integrated iron and steel industry zone compared with a background site. Aerosol Air Qual. Res. 15, 875–887. https://doi.org/10.4209/aaqr.2014.09.0226

Dai, Q., Bi, X., Song, W., Li, T., Liu, B., Ding, J., Xu, J., Song, C., Yang, N., Schulze, B.C., Zhang, Y., Feng, Y., Hopke, P.K. (2019). Residential coal combustion as a source of primary sulfate in Xi'an, China. Atmos. Environ. 196, 66–76. https://doi.org/10.1016/j.atmosenv.2018.10.002

Dai, Q., Liu, B., Bi, X., Wu, J., Liang, D., Zhang, Y., Feng, Y., Hopke, P.K. (2020). Dispersion normalized PMF provides insights into the significant changes in source contributions to $PM_{2.5}$ after the COVID-19 Outbreak. Environ. Sci. Technol. 54, 9917–9927. https://doi.org/10.1021/acs.est.0c02776

Dai, Q., Ding, J., Hou, L., Li, L., Cai, Z., Liu, B., Song, C., Bi, X., Wu, J., Zhang, Y., Feng, Y., Hopke, P.K. (2021). Haze episodes before and during the COVID-19 shutdown in Tianjin, China: Contribution of fireworks and residential burning. Environ. Pollut. 286, 117252. https://doi.org/10.1016/j.envpol.2021.117252

Dai, Q., Chen, J., Wang, X., Dai, T., Tian, Y., Bi, X., Shi, G., Wu, J., Liu, B., Zhang, Y., Yan, B., Kinney, P.L., Feng, Y., Hopke, P.K. (2023). Trends of source apportioned $PM_{2.5}$ in Tianjin over 2013–2019: Impacts of clean air actions. Environ. Pollut. 325, 121344. https://doi.org/10.1016/j.envpol.2023.121344

Enghag, P. (2008). Encyclopedia of the Elements: Technical Data - History - Processing - Applications. John Wiley & Sons, NJ, Hoboken.

Global Energy Monitor (2022). Global coal plant tracker. https://globalenergymonitor.org/projects/global-coal-plant-tracker/tracker/ (accessed 14 May 2022).

Griffith, S.M., Huang, W.S., Lin, C.C., Chen, Y.C., Chang, K.E., Lin, T.H., Wang, S.H., Lin, N.H. (2020). Long-range air pollution transport in East Asia during the first week of the COVID-19 lockdown in China. Sci. Total Environ. 741, 140214. https://doi.org/10.1016/j.scitotenv.2020.140214

Gunthe, S.S., Liu, P., Panda, U., Raj, S.S., Sharma, A., Darbyshire, E., Reyes-Villegas, E., Allan, J., Chen, Y., Wang, X., Song, S., Pöhlker, M.L., Shi, L., Wang, Y., Kommula, S.M., Liu, T., Ravikrishna, R., McFiggans, G., Mickley, L.J., Martin, S.T., *et al.* (2021). Enhanced aerosol particle growth sustained by high continental chlorine emission in India. Nat. Geosci. 14, 77–84. https://doi.org/10.1038/s41561-020-00677-x

Han, Y.J. (2005). Identification of possible mercury sources and estimation of mercury wet deposition flux in Lake Ontario from Lake Ontario atmospheric deposition study (LOADS). Environ. Eng. Res. 10, 306–315. https://doi.org/10.4491/eer.2005.10.6.306

Heo, J.B., Hopke, P.K., Yi, S.M. (2009). Source apportionment of $PM_{2.5}$ in Seoul, Korea. Atmos. Chem. Phys. 9, 4957–4971. https://doi.org/10.5194/acp-9-4957-2009

Hopke, P.K. (2016). Review of receptor modeling methods for source apportionment. J. Air Waste Manage. Assoc. 66, 237–259. https://doi.org/10.1080/10962247.2016.1140693

Hopke, P.K., Dai, Q., Li, L., Feng, Y. (2020). Global review of recent source apportionments for airborne particulate matter. Sci. Total Environ. 740, 140091. https://doi.org/10.1016/j.scitotenv.2020.140091

Hung, W.T., Lu, C.H., Wang, S.H., Chen, S.P., Tsai, F., Chou, C.C.K. (2019). Investigation of long-range transported $PM_{2.5}$ events over Northern Taiwan during 2005–2015 winter seasons. Atmo. Environ. 217, 116920. https://doi.org/10.1016/j.atmosenv.2019.116920

International Energy Agency (IEA) (2019). The Future of Cooling in China, IEA, Paris. https://www.iea.org/reports/the-future-of-cooling-in-china

Islam, N., Toha, T.R., Islam, M.M., Ahmed, T. (2023). Spatio-temporal variation of meteorological influence on $PM_{2.5}$ and PM_{10} over major urban cities of Bangladesh. Aerosol Air Qual. Res. 23, 220082. https://doi.org/10.4209/AAQR.220082

Jang, H.N., Seo, Y.C., Lee, J.H., Hwang, K.W., Yoo, J.I., Sok, C.H., Kim, S.H. (2007). Formation of fine particles enriched by V and Ni from heavy oil combustion: Anthropogenic sources and drop-tube furnace experiments. Atmos. Environ. 41, 1053–1063. https://doi.org/10.1016/j.atmosenv.2006.09.011

Jayarathne, T., Stockwell, C.E., Bhave, P.V., Praveen, P.S., Rathnayake, C.M., Islam, M.R., Panday, A.K., Adhikari, S., Maharjan, R., Goetz, J.D., DeCarlo, P.F., Saikawa, E., Yokelson, R.J., Stone, E.A. (2018). Nepal Ambient Monitoring and Source Testing Experiment (NAMaSTE): emissions of particulate matter from wood- and dung-fueled cooking fires, garbage and crop residue burning, brick kilns, and other sources. Atmos. Chem. Phys. 18, 2259–2286. https://doi.org/10.5194/acp-18-2259-2018

Kai, K., Kawai, K., Ito, A., Aizawa, Y., Minamoto, Y., Munkhjargal, E., Davaanyam, E. (2021). Dust hotspot in the gobi desert: A field survey in April 2019. Sola 17, 130–133. https://doi.org/10.2151/sola.2021-023

Keeler, G.J. (1987). A hybrid approach for source apportionment of atmospheric pollutants in the northeastern United States. Ph.D. dissertation, University of Michigan, USA.

Kim, E., Hopke, P.K. (2008). Source characterization of ambient fine particles at multiple sites in the Seattle area. Atmos. Environ. 42, 6047–6056. https://doi.org/10.1016/j.atmosenv.2008.03.032

Kim, H., Zhang, Q., Sun, Y. (2020a). Measurement report: Characterization of severe spring haze episodes and influences of long-range transport in the Seoul metropolitan area in March 2019. Atmos. Chem. Phys. 20, 11527–11550. https://doi.org/10.5194/acp-20-11527-2020

Kim, J.H., Lim, A.Y., Cheong, H.K. (2020b). Trends of accidental carbon monoxide poisoning in Korea, 1951-2018. Epidemiol. Health 42, e2020062. https://doi.org/10.4178/epih.e2020062

Kim, J.Y., Song, C.H., Ghim, Y.S., Won, J.G., Yoon, S.C., Carmichael, G.R., Woo, J.H. (2006). An investigation on NH_3 emissions and particulate NH_4^+–NO_3^- formation in East Asia. Atmos. Environ. 40, 2139–2150. https://doi.org/10.1016/j.atmosenv.2005.11.048

Kim, S., Kim, T.Y., Yi, S.M., Heo, J. (2018). Source apportionment of $PM_{2.5}$ using positive matrix factorization (PMF) at a rural site in Korea. J. Environ. Manage. 214, 325–334. https://doi.org/10.1016/j.jenvman.2018.03.027

Kim, Y., Jeon, K., Park, J., Shim, K., Kim, S.W., Shin, H.J., Yi, S.M., Hopke, P.K. (2022a). Local and transboundary impacts of $PM_{2.5}$ sources identified in Seoul during the early stage of the COVID-19 outbreak. Atmos. Pollut. Res. 13, 101510. https://doi.org/10.1016/j.apr.2022.101510

Kim, Y., Kim, H., Kang, H., de Foy, B., Zhang, Q. (2022b). Impacts of secondary aerosol formation and long range transport on severe haze during the winter of 2017 in the Seoul metropolitan area. Sci. Total Environ. 804, 149984. https://doi.org/10.1016/j.scitotenv.2021.149984

Korea Environment Corporation (2017). The 5th survey on national waste (2016 – 2017). Korea Environment Corporation, Korea.

Korea Meteorological Administration (KMA) (2021). Open MET Data Portal. National Climate Data Center. https://data.kma.go.kr/data/grnd/selectAwsRltmList.do?pgmNo=56

Korea Meteorological Administration (KMA) (2022). Observation days of Asian dust. https://www.weather.go.kr/w/dust/dust-obs-days.do?type=1&stnId=152 (accessed 5 December 2022).

Kumar, S., Aggarwal, S.G., Sarangi, B., Malherbe, J., Barre, J.P.G., Berail, S., Séby, F., Donard, O.F.X. (2018). Understanding the influence of open-waste burning on urban aerosols using metal tracers and lead isotopic composition. Aerosol Air Qual. Res. 18, 2433–2446. https://doi.org/10.4209/aaqr.2017.11.0510

Lee, B.K., Hieu, N.T. (2011). Seasonal variation and sources of heavy metals in atmospheric aerosols in a residential area of Ulsan, Korea. Aerosol Air Qual. Res. 11, 679–688. https://doi.org/10.4209/aaqr.2010.10.0089

Lee, J.H., Hopke, P.K., Turner, J.R. (2006). Source identification of airborne $PM_{2.5}$ at the St. Louis-Midwest Supersite. J. Geophys. Res. 111, D10S10. https://doi.org/10.1029/2005JD006329

Lee, K., Chandra, I., Seto, T., Inomata, Y., Hayashi, M., Takami, A., Yoshino, A., Otani, Y. (2019). Aerial observation of atmospheric nanoparticles on Fukue Island, Japan. Aerosol Air Qual. Res. 19, 981–994. https://doi.org/10.4209/aaqr.2018.03.0077

Lee, Y., Won, S.R., Shin, H.J., Kim, D.G., Lee, J.Y. (2023). Seasonal characteristics of volatile organic compounds in Seoul, Korea: Major sources and contribution to secondary organic aerosol formation. Aerosol Air Qual. Res. 23, 220429. https://doi.org/10.4209/aaqr.220429

Lewis, C.W., Norris, G.A., Conner, T.L., Henry, R.C. (2003). Source apportionment of phoenix $PM_{2.5}$ aerosol with the unmix receptor model. J. Air Waste Manage. Assoc. 53, 325–338. https://doi.org/10.1080/10473289.2003.10466155

Li, G., Lei, W., Bei, N., Molina, L.T. (2012). Contribution of garbage burning to chloride and $PM_{2.5}$ in Mexico City. Atmos. Chem. Phys. 12, 8751–8761. https://doi.org/10.5194/acp-12-8751-2012

Li, X., Yang, K., Han, J., Ying, Q., Hopke, P.K. (2019). Sources of humic-like substances (HULIS) in $PM_{2.5}$ in Beijing: Receptor modeling approach. Sci. Total Environ. 671, 765–775. https://doi.org/10.1016/j.scitotenv.2019.03.333

Lioy, P.J., Zelenka, M.P., Cheng, M.D., Reiss, N.M., Wilson, W.E. (1989). The effect of sampling duration on the ability to resolve source types using factor analysis. Atmos. Environ. 23, 239–254. https://doi.org/10.1016/0004-6981(89)90116-9

Liu, B., Wu, J., Zhang, J., Wang, L., Yang, J., Liang, D., Dai, Q., Bi, X., Feng, Y., Zhang, Y., Zhang, Q. (2017). Characterization and source apportionment of $PM_{2.5}$ based on error estimation from EPA PMF 5.0 model at a medium city in China. Environ. Pollut. 222, 10–22. https://doi.org/10.1016/j.envpol.2017.01.005

Liu, E., Yan, T., Birch, G., Zhu, Y. (2014). Pollution and health risk of potentially toxic metals in urban road dust in Nanjing, a mega-city of China. Sci. Total Environ. 476–477, 522–531. https://doi.org/10.1016/j.scitotenv.2014.01.055

Liu, S., Xing, J., Wang, S., Ding, D., Chen, L., Hao, J. (2020). Revealing the impacts of transboundary pollution on $PM_{2.5}$-related deaths in China. Environ. Int. 134, 105323. https://doi.org/10.1016/j.envint.2019.105323

Liu, Y., Fan, Q., Chen, X., Zhao, J., Ling, Z., Hong, Y., Li, W., Chen, X., Wang, M., Wei, X. (2018). Modeling the impact of chlorine emissions from coal combustion and prescribed waste incineration on tropospheric ozone formation in China. Atmos. Chem. Phys. 18, 2709–2724. https://doi.org/10.5194/acp-18-2709-2018

Maxwell-Meier, K., Weber, R., Song, C., Orsini, D., Ma, Y., Carmichael, G.R., Streets, D.G. (2004). Inorganic composition of fine particles in mixed mineral dust–pollution plumes observed from airborne measurements during ACE-Asia. J. Geophys. Res. 109, D19S07. https://doi.org/10.1029/2003JD004464

Miyakawa, T., Takegawa, N., Kondo, Y. (2007). Removal of sulfur dioxide and formation of sulfate aerosol in Tokyo. J. Geophys. Res. 112, D13209. https://doi.org/10.1029/2006JD007896

Moffet, R.C., Desyaterik, Y., Hopkins, R.J., Tivanski, A.V., Gilles, M.K., Wang, Y., Shutthanandan, V., Molina, L.T., Abraham, R.G., Johnson, K.S., Mugica, V., Molina, M.J., Laskin, A., Prather, K.A. (2008). Characterization of aerosols containing Zn, Pb, and Cl from an industrial region of Mexico City. Environ. Sci. Technol. 42, 7091–7097. https://doi.org/10.1021/es7030483

Monks, P.S., Granier, C., Fuzzi, S., Stohl, A., Williams, M.L., Akimoto, H., Amann, M., Baklanov, A., Baltensperger, U., Bey, I., Blake, N., Blake, R.S., Carslaw, K., Cooper, O.R., Dentener, F., Fowler, D., Fragkou, E., Frost, G.J., Generoso, S., Ginoux, P., *et al.* (2009). Atmospheric composition change – global and regional air quality. Atmos. Environ. 43, 5268–5350. https://doi.org/10.1016/j.atmosenv.2009.08.021

National Bureau of Statistics of China (2022). Volume of Freight Handled in Coastal Ports. National data. https://data.stats.gov.cn/englisheasyquery.htm?cn=A0 (accessed 14 May 2022).

Norris, G., Duvall, R., Brown, S., Bai, S. (2014). EPA Positive Matrix Factorization 5.0 Fundamentals and User Guide. U.S. Environmental Protection Agency, USA. https://www.epa.gov/sites/default/files/2015-02/documents/pmf_5.0_user_guide.pdf

Paatero, P., Tapper, U. (1994). Positive matrix factorization: A non-negative factor model with optimal utilization of error estimates of data values. Environmetrics 5, 111–126. https://doi.org/10.1002/env.3170050203

Paatero, P., Hopke, P.K. (2003). Discarding or downweighting high-noise variables in factor analytic models. Anal. Chim. Acta 490, 277–289. https://doi.org/10.1016/S0003-2670(02)01643-4

Paatero, P., Hopke, P.K., Begum, B.A., Biswas, S.K. (2005). A graphical diagnostic method for assessing the rotation in factor analytical models of atmospheric pollution. Atmos. Environ. 39, 193–201. https://doi.org/10.1016/j.atmosenv.2004.08.018

Paatero, P., Eberly, S., Brown, S.G., Norris, G.A. (2014). Methods for estimating uncertainty in factor analytic solutions. Atmos. Meas. Tech. 7, 781–797. https://doi.org/10.5194/amt-7-781-2014

Park, E.H., Heo, J., Hirakura, S., Hashizume, M., Deng, F., Kim, H., Yi, S.M. (2018). Characteristics of $PM_{2.5}$ and its chemical constituents in Beijing, Seoul, and Nagasaki. Air Qual. Atmos. Health 11, 1167–1178. https://doi.org/10.1007/s11869-018-0616-y

Park, J., Lee, K.H., Kim, H., Woo, J., Heo, J., Jeon, K., Lee, C.H., Yoo, C.G., Hopke, P.K., Koutrakis, P., Yi, S.M. (2024). Analysis of $PM_{2.5}$ inorganic and organic constituents to resolve contributing sources in Seoul, South Korea and Beijing, China and their possible associations with cytokine IL-8. Environ. Res. 243, 117860. https://doi.org/10.1016/j.envres.2023.117860

Park, R.J., Jacob, D.J., Field, B.D., Yantosca, R.M., Chin, M. (2004). Natural and transboundary pollution influences on sulfate-nitrate-ammonium aerosols in the United States: Implications for policy. J. Geophys. Res. 109, D15204. https://doi.org/10.1029/2003JD004473

Peng, J., Hu, M., Shang, D., Wu, Z., Du, Z., Tan, T., Wang, Y., Zhang, F., Zhang, R. (2021). Explosive secondary aerosol formation during severe haze in the North China Plain. Environ. Sci. Technol. 55, 2189–2207. https://doi.org/10.1021/acs.est.0c07204

Perry, K.D., Cahill, T.A., Eldred, R.A., Dutcher, D.D., Gill, T.E. (1997). Long-range transport of North African dust to the eastern United States. J. Geophys. Res. 102, 11225–11238. https://doi.org/10.1029/97JD00260

Raspisaniye Pogodi Ltd. (2021). Weather for 243 countries of the world. https://rp5.ru/Weather_in_the_world

Shanavas, A.K., Zhou, C., Menon, R., Hopke, P.K. (2020). PM_{10} source identification using the trajectory based potential source apportionment (TraPSA) toolkit at Kochi, India. Atmos. Pollut. Res. 11, 1535–1542. https://doi.org/10.1016/j.apr.2020.06.019

Sillanpää, M., Hillamo, R., Saarikoski, S., Frey, A., Pennanen, A., Makkonen, U., Spolnik, Z., Van Grieken, R., Braniš, M., Brunekreef, B., Chalbot, M.C., Kuhlbusch, T., Sunyer, J., Kerminen, V.M., Kulmala, M., Salonen, R.O. (2006). Chemical composition and mass closure of particulate matter at six urban sites in Europe. Atmos. Environ. 40, 212–223. https://doi.org/10.1016/j.atmosenv.2006.01.063

Song, L., Yin, S., Bi, S., Yang, J., Wang, X., Bi, X., Zhang, Y., Wu, J., Dai, Q., Feng, Y. (2024). More evidence on primary sulfate emission from residential coal combustion in northern China: Insights from the size-segregated chemical profile, morphology, and sulfur isotope. Atmos. Environ. 326, 120467. https://doi.org/10.1016/j.atmosenv.2024.120467

Statistics Korea (2022). ship's entry and departure. Korean Statistical Information Service. https://kosis.kr/statHtml/statHtml.do?orgId=146&tblId=DT_MLTM_1298&conn_path=I3 (accessed 14 May 2022).

Stein, A.F., Draxler, R.R., Rolph, G.D., Stunder, B.J.B., Cohen, M.D., Ngan, F. (2015). NOAA's HYSPLIT atmospheric transport and dispersion modeling system. Bull. Am. Meteorol. Soc. 96, 2059–2077. https://doi.org/10.1175/BAMS-D-14-00110.1

Su, L., Yuan, Z., Fung, J.C.H., Lau, A.K.H. (2015). A comparison of HYSPLIT backward trajectories generated from two GDAS datasets. Sci. Total Environ. 506–507, 527–537. https://doi.org/10.1016/j.scitotenv.2014.11.072

Tan, S.C., Li, J., Che, H., Chen, B., Wang, H. (2017). Transport of East Asian dust storms to the marginal seas of China and the southern North Pacific in spring 2010. Atmos. Environ. 148, 316–328. https://doi.org/10.1016/j.atmosenv.2016.10.054

Tang, Y., Han, S., Yao, Q., Cai, Z., Qiu, Y., Feng, J. (2020). Analysis of a severe regional haze-fog-dust episode over north China in autumn by using multiple observation data. Aerosol Air Qual. Res. 20, 2211–2225. https://doi.org/10.4209/aaqr.2019.11.0567

Tian, H., Liu, K., Zhou, J., Lu, L., Hao, J., Qiu, P., Gao, J., Zhu, C., Wang, K., Hua, S. (2014). Atmospheric emission inventory of hazardous trace elements from China's coal-fired power plants—Temporal trends and spatial variation characteristics. Environ. Sci. Technol. 48, 3575–3582. https://doi.org/10.1021/es404730j

Tian, H.Z., Zhu, C.Y., Gao, J.J., Cheng, K., Hao, J.M., Wang, K., Hua, S.B., Wang, Y., Zhou, J.R. (2015). Quantitative assessment of atmospheric emissions of toxic heavy metals from anthropogenic sources in China: historical trend, spatial distribution, uncertainties, and control policies. Atmos. Chem. Phys. 15, 10127–10147. https://doi.org/10.5194/acp-15-10127-2015

UCL Energy Institute (2021). Movements of the global merchant fleet over the course of 2012. https://www.shipmap.org/ (accessed 14 May 2022).

Uno, I., Eguchi, K., Yumimoto, K., Takemura, T., Shimizu, A., Uematsu, M., Liu, Z., Wang, Z., Hara, Y., Sugimoto, N. (2009). Asian dust transported one full circuit around the globe. Nat. Geosci. 2, 557–560. https://doi.org/10.1038/ngeo583

Uria-Tellaetxe, I., Carslaw, D.C. (2014). Conditional bivariate probability function for source identification. Environ. Modell. Software 59, 1–9. https://doi.org/10.1016/j.envsoft.2014.05.002

Vallius, M., Janssen, N.A.H., Heinrich, J., Hoek, G., Ruuskanen, J., Cyrys, J., Van Grieken, R., De Hartog, J.J., Kreyling, W.G., Pekkanen, J. (2005). Sources and elemental composition of ambient $PM_{2.5}$ in three European cities. Sci. Total Environ. 337, 147–162. https://doi.org/10.1016/j.scitotenv.2004.06.018

VanCuren, R.A., Cahill, T.A. (2002). Asian aerosols in North America: Frequency and concentration of fine dust. J. Geophys. Res. 107, 4804. https://doi.org/10.1029/2002JD002204

Vouk, V.B., Piver, W.T. (1983). Metallic elements in fossil fuel combustion products: amounts and form of emissions and evaluation of carcinogenicity and mutagenicity. Environ. Health Perspect. 47, 201–225. https://doi.org/10.1289/ehp.8347201

Wang, G., Zhang, R., Gomez, M.E., Yang, L., Levy Zamora, M., Hu, M., Lin, Y., Peng, J., Guo, S., Meng, J., Li, J., Cheng, C., Hu, T., Ren, Y., Wang, Y., Gao, J., Cao, J., An, Z., Zhou, W., Li, G., *et al.* (2016). Persistent sulfate formation from London Fog to Chinese haze. Proc. Natl. Acad. Sci. U.S.A. 113, 13630–13635. https://doi.org/10.1073/pnas.1616540113

Wang, L., Liu, Z., Sun, Y., Ji, D., Wang, Y. (2015). Long-range transport and regional sources of $PM_{2.5}$ in Beijing based on long-term observations from 2005 to 2010. Atmos. Res. 157, 37–48. https://doi.org/10.1016/j.atmosres.2014.12.003

Wang, Y., Gong, Y., Bai, C., Yan, H., Yi, X. (2023). Exploring the convergence patterns of $PM_{2.5}$ in Chinese cities. Environ. Dev. Sustain. 25, 708–733. https://doi.org/10.1007/s10668-021-02077-6

Whisman, M.L., Goetzinger, J.W., Cotton, F.O. (1974). Waste Lubricating Oil Research: A Comparison of Bench-test Properties of Re-refined and Virgin Lubricating Oils. U.S. Bureau of Mines, USA.

World Health Organization (WHO) (2016). Ambient (outdoor) air pollution. https://www.who.int/news-room/fact-sheets/detail/ambient-(outdoor)-air-quality-and-health (accessed 7 November 2022).

World Health Organization (WHO) (2021). WHO global air quality guidelines: particulate matter ($PM_{2.5}$ and PM_{10}), ozone, nitrogen dioxide, sulfur dioxide and carbon monoxide. World Health Organization, Geneva. https://www.who.int/publications/i/item/9789240034228

World Shipping Council (2020). The Top 50 Container Ports. https://www.worldshipping.org/top-50-ports

Xie, Y., Liu, Z., Wen, T., Huang, X., Liu, J., Tang, G., Yang, Y., Li, X., Shen, R., Hu, B., Wang, Y. (2019). Characteristics of chemical composition and seasonal variations of $PM_{2.5}$ in Shijiazhuang, China: Impact of primary emissions and secondary formation. Sci. Total Environ. 677, 215–229. https://doi.org/10.1016/j.scitotenv.2019.04.300

Yang, H.H., Luo, S.W., Lee, K.T., Wu, J.Y., Chang, C.W., Chu, P.F. (2016). Fine particulate speciation profile and emission factor of municipal solid waste incinerator established by dilution sampling method. J. Air Waste Manage. Assoc. 66, 807–814. https://doi.org/10.1080/10962247.2016.1184195

Yen, P.H., Yuan, C.S., Soong, K.Y., Jeng, M.S., Cheng, W.H. (2024). Identification of potential source regions and long-range transport routes/channels of marine $PM_{2.5}$ at remote sites in East Asia. Sci. Total Environ. 915, 170110. https://doi.org/10.1016/j.scitotenv.2024.170110

Yu, L., Wang, G., Zhang, R., Zhang, L., Song, Y., Wu, B., Li, X., An, K., Chu, J. (2013). Characterization and source apportionment of $PM_{2.5}$ in an urban environment in Beijing. Aerosol Air Qual. Res. 13, 574–583. https://doi.org/10.4209/aaqr.2012.07.0192

Yu, Y., Li, Y., Li, B., Shen, Z., Stenstrom, M.K. (2016). Metal enrichment and lead isotope analysis for source apportionment in the urban dust and rural surface soil. Environ. Pollut. 216, 764–772. https://doi.org/10.1016/j.envpol.2016.06.046

Zannoni, D., Valotto, G., Visin, F., Rampazzo, G. (2016). Sources and distribution of tracer elements in road dust: The Venice mainland case of study. J. Geochem. Explor. 166, 64–72. https://doi.org/10.1016/j.gexplo.2016.04.007

Zhao, J., Zhang, Y., Xu, H., Tao, S., Wang, R., Yu, Q., Chen, Y., Zou, Z., Ma, W. (2021). Trace elements from ocean-going vessels in East Asia: Vanadium and nickel emissions and their impacts on air quality. J. Geophys. Res. 126, e2020JD033984. https://doi.org/10.1029/2020JD033984

Zhou, C., Zhou, H., Hopke, P.K., Holsen, T.M. (2024). Overview of the trajectory-ensemble

potential source apportionment web (TraPSA-Web) toolkit for atmospheric pollutant source identification. Atmosphere 15, 176. https://doi.org/10.3390/atmos15020176

Zhou, L., Hopke, P.K., Liu, W. (2004). Comparison of two trajectory based models for locating particle sources for two rural New York sites. Atmos. Environ. 38, 1955–1963. https://doi.org/10.1016/j.atmosenv.2003.12.034

Zhou, R., Yan, C., Cui, M., Xu, M., Liu, W., Chen, H., Zhou, T., Zheng, M. (2021). Research status and prospects on source apportionment of atmospheric fine particulate matter in Shandong Province. China Environ. Sci. 41, 3029–3042. http://www.zghjkx.com.cn/CN/Y2021/V41/I7/3029 (in Chinese)